

# Influence of superimposed biaxial stress on the tensile strength of perfect crystals from first principles

Miroslav Černý\* and Jaroslav Pokluda

*Institute of Engineering Physics, Faculty of Mechanical Engineering, Brno University of Technology,  
Technická 2, CZ-616 69 Brno, Czech Republic*

(Received 16 March 2007; revised manuscript received 21 May 2007; published 30 July 2007)

Influence of biaxial stresses applied perpendicularly to the [100] loading axis on the theoretical tensile strength is studied from first principles. Ten crystals of cubic metals and three crystals of diamond ceramics were selected as particular case studies. Obtained results show that, within a limited range of biaxial stresses, the tensile strength monotonously increases with increasing biaxial tensile stress for most of the studied metals. Within the range, the dependence can be approximated by a linear function. Beyond the range, the dependence shows a maximum that usually appears in the tensile range of biaxial stresses. On the other hand, some of the materials (Si, Ni, Cu, and Ge) exhibit a maximum tensile strength at nearly uniaxial stress state, and the superposition of both tensile and compressive biaxial stresses reduces the tensile strength. Unlike the other crystals, diamond revealed a maximum under compressive biaxial stress.

DOI: [10.1103/PhysRevB.76.024115](https://doi.org/10.1103/PhysRevB.76.024115)

PACS number(s): 62.20.-x, 61.66.Bi, 81.40.Jj, 71.15.Mb

## I. INTRODUCTION

Calculations of the theoretical (ideal) strength of materials and investigations on micromechanisms of materials failure are motivated by the development of new materials exhibiting better mechanical properties. Although there is no doubt that crystals and whiskers used in the industrial exploitation are usually subjected to a multiaxial loading, little attention has been paid to a coupling of various stress tensor components. Several studies were focused on the influence of superimposed hydrostatic or normal stress on the theoretical shear strength.<sup>1-3</sup> The results reveal an increase in the shear strength with increasing compressive normal (triaxial) stress. Such analyses allow us, for example, to localize the very onset of plastic deformation under the nanoindenter (dislocation emissions) and, consequently, yield a deeper insight into the physical nature of damage processes.<sup>1,4</sup> Another example of high practical importance is associated with reinforcing fibers used in engineering composite materials. Due to the matrix/reinforcement incompatibility strain, the single crystal fibers (or whiskers) are subjected to multiaxial loading even in the case of remote purely uniaxial tension of the composite material. Consequently, *ab initio* modeling of the tension of perfect crystals under superimposed tensile or compressive biaxial stresses is expected to be a reasonable theoretical simulation of the stress-strain behavior of fibers in the composite.

This work examines the effect of the superimposed biaxial stress on the [100] stress-strain response of crystals and, in particular, on the theoretical tensile strength (TTS). Besides the practical impact, the motivation for the research was also based on our previous experience with calculations of the theoretical strength under isotropic tension and compression<sup>5-8</sup> as well as those of TTS under conditions preventing the Poisson contraction (performed by other authors<sup>9</sup>). For some crystals, higher values of TTS were predicted in the case of superimposed tensile biaxial stresses. A previous study for the iron crystal<sup>10</sup> has also revealed that a superimposed hydrostatic tension (compression) raises (lowers) the ideal tensile strength relative to the uniaxial case.

## II. COMPUTATIONAL DETAILS

For the electronic structure calculations, we utilized the Vienna *Ab initio* Simulation Package (VASP).<sup>11,12</sup> This code uses the plane-wave basis set and the projector augmented-wave potential<sup>13</sup> or ultrasoft pseudopotentials of Vanderbilt type.<sup>14</sup> The exchange-correlation energy was evaluated using the local density approximation (LDA) or the generalized-gradient approximation (GGA) of Perdew and Wang.<sup>15</sup> Spin-polarized calculations were performed for Ni and Fe to include the collinear ferromagnetism into the calculations. After proper convergence tests,  $18 \times 18 \times 18$   $k$ -point mesh was found to be satisfactory for most of the studied metals. An energy cutoff ( $E_{cut}$ ) of the plane-wave expansion was increased in order to obtain correct stress values. The solution was considered to be self-consistent when the energy difference of two consequent iterations was smaller than  $10 \mu\text{eV}$ .

The calculation procedure based on the VASP code was applied to ten cubic crystals (V, Fe, Ni, Cu, Nb, Mo, W, Ir, Pt, and Au) and three crystals of a diamond structure (C, Si, and Ge). All studied crystalline systems were subjected to the tensile stress  $\sigma_{uni}$  along the [100] direction combined with the transverse biaxial stresses  $\sigma_{bi}$  in the (100) plane. A relaxation procedure based on Hellman-Feynman forces in (100) plane was applied in order to get the stress tensor in the simple form

$$\hat{\sigma} = \begin{vmatrix} \sigma_{uni} & 0 & 0 \\ 0 & \sigma_{bi} & 0 \\ 0 & 0 & \sigma_{bi} \end{vmatrix}.$$

The relaxation process consisted of the following steps: (i) The crystal was subjected to  $\sigma_{bi}$  of a certain preset value (the edges perpendicular to the [100] direction were allowed to change their lengths in order to converge  $\sigma_{bi}$  to the preset value). (ii) The crystal was incrementally elongated in the [100] direction and the value of  $\sigma_{bi}$  was converged to the same preset value for any elongation. During the simulated deformation process, the  $\sigma_{uni}$  values were not directly con-

TABLE I. Computed values of the equilibrium lattice parameter  $a_0$  and Young's modulus  $E_{100}$  along with experimental values. The table also contains utilized computational parameters such as the exchange-correlation approximation (XC) and the plane-wave energy cutoff ( $E_{cut}$ ).

Crystal		$a_0$ (Å)		$E_{100}$ (GPa)		XC	$E_{cut}$ (eV)
		Calc.	Expt.	Calc.	Expt.		
C	dia	3.53	3.57	1065	1050	LDA	370
Si	dia	5.39	5.43	126	130	LDA	190
Ge	dia	5.75	5.66	98.6	104	LDA	373
V	bcc	2.99	3.03	178	151	GGA	342
Fe	bcc	2.83	2.87	173	143	GGA	350
Ni	fcc	3.52	3.52	157	151	GGA	350
Cu	fcc	3.64	3.61	76.9	72.6	GGA	355
Nb	bcc	3.29	3.30	147	152	GGA	290
Mo	bcc	3.15	3.15	397	394	GGA	290
W	bcc	3.17	3.16	423	417	GGA	290
Ir	fcc	3.88	3.84	434	438	GGA	257
Pt	fcc	3.91	3.92	149	136	LDA	260
Au	fcc	4.07	4.08	48.1	46.5	LDA	230

trolled by our relaxation procedure. Consequently, they reflect the changes of applied [100] strain  $\varepsilon_{uni}$ . (iii) The stress maximum  $\sigma_{max}$  and the related strain  $\varepsilon_{max}$  were found by a cubic spline interpolation of computed  $\sigma_{uni}$  values. If no other instability precedes, the  $\sigma_{max}$  value can be considered to be the theoretical tensile strength under corresponding superimposed biaxial stresses. (iv) The relaxation procedure was repeated for several preset  $\sigma_{bi}$  values.

Some of the previous studies of the crystal stability under uniaxial loading reported shear<sup>9,16–18</sup> or phonon<sup>19</sup> instabilities before reaching the maximum computed uniaxial stress (the point of inflection on the dependence of the crystal energy on  $\varepsilon_{uni}$ ). This obviously means a reduction of the tensile strength. On the other hand, crystals of some elements under [100] uniaxial loading were found to remain stable with respect to shear until  $\sigma_{uni}$  reached its maximum.<sup>16,20</sup> Other authors that have employed the elastic stability theory with molecular dynamics simulations (nonzero temperature) have observed instabilities at smaller stresses than predicted by static-type (zero temperature) calculations.<sup>21–23</sup>

### III. COMPUTED RESULTS AND DISCUSSION

#### A. Ground state properties

In order to check the reliability of both the relaxation procedure and the computational code (with the utilized parameters), we applied the relaxation procedure also for a calculation of the equilibrium lattice parameter  $a_0$  (converged until  $\sigma_{uni} = \sigma_{bi} \leq 0.02$  GPa) and Young's modulus  $E_{100}$  ( $\sigma_{bi} \leq 0.02$  GPa).

The computed  $a_0$  ( $1 \text{ Å} = 10^{-10} \text{ m}$ ) and  $E_{100}$  values are listed in Table I together with available experimental data.<sup>24</sup>

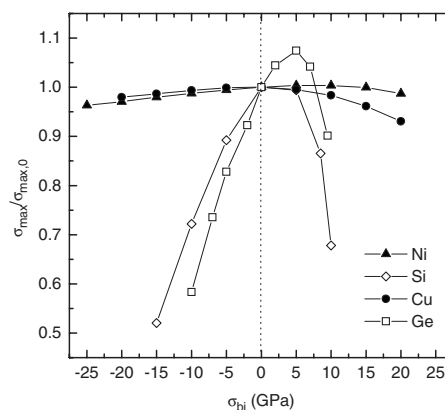


FIG. 1. Normalized values of the theoretical tensile strength  $\sigma_{max}/\sigma_{max,0}$  as functions of superimposed biaxial stress  $\sigma_{bi}$  for Si, Ge, Ni, and Cu.

The experimental  $E_{100}$  value for diamond was taken from Ref. 25 and the other  $E_{100}$  values in the column were obtained from experimental elastic constants<sup>26</sup> using the following relation:<sup>27</sup>

$$E_{100} = \frac{(C_{11} - C_{12})(C_{11} + 2C_{12})}{C_{11} + C_{12}}.$$

As can be seen from Table I, the  $a_0$  values correspond well to experimental data (mostly within 1%). Also the calculated values of  $E_{100}$  are very reasonable except for those of V and Fe. The most significant overestimation (20%) can be seen for ferromagnetic iron. On the other hand, our value is even 5% lower than results of Clatterbuck *et al.*<sup>20</sup>

#### B. Theoretical strength

Atomistic modeling of the tensile test was performed under the superimposed biaxial stresses within the range of  $\pm 25$  GPa with the exception of crystals exhibiting low values of the plane strength. All the stresses calculated in this work represent values of the true stress (the axial force divided by the true area in the stressed state).

Rather anomalous dependences of the normalized strength value  $\sigma_{max}/\sigma_{max,0}$  on  $\sigma_{bi}$  (within the studied range) are shown in Fig. 1, as received for four elements Ni, Cu, Si, and Ge. The values of  $\sigma_{max,0}$  correspond to computed  $\sigma_{max}$  values under pure uniaxial tension. The most remarkable influence of  $\sigma_{bi}$  can be observed in the case of Ge and Si. The applied biaxial stress (both tensile and compressive) substantially reduces the TTS of those crystals. The maxima of displayed curves for Si and Cu lie close to the state of zero biaxial stresses ( $0 < \sigma_{bi} < 3$  GPa), while in the case of Ge and Ni, the maxima are associated with somewhat higher  $\sigma_{bi}$  of about 5 and 8 GPa, respectively.

Previous calculations of TTS for Ni and Cu (Ref. 28) yielded lower values in the case when Poisson contraction was omitted ([100] deformation) than in the case of transverse relaxation ([100] loading). By applying the uniaxial ultimate strain  $\varepsilon_{max,0}$  to a system without Poisson contraction, our calculations yield  $\sigma_{bi}$  values of 18 and 13 GPa for Ni and Cu, respectively. The related  $\sigma_{uni}$  values of 34.8 and

TABLE II. Slope of the linear regression lines  $k=d\sigma_{max}/d\sigma_{bi}$ , the maximum stress  $\sigma_{max,0}$  (GPa), and the ultimate strain  $\epsilon_{max,0}$  under pure uniaxial loading along with available literature data and computed values of the theoretical isotropic strength  $\sigma_{iso}$  (GPa).

	$\sigma_{max,0}$	$k_{max}$	$\epsilon_{max,0}$	TTS	$\sigma_{iso}$
C	225	-1.08	0.37	225 <sup>a</sup>	88.5
Si	26.3		0.26		15.5
Ge	16.8		0.23		11.1
V	19.8	0.688	0.22		32.7
Fe	12.4	0.634	0.16	14.2 <sup>b</sup>	27.7
Ni	35.2		0.37	39.0 <sup>c</sup>	28.9
Cu	24.1		0.36	23.7 <sup>c</sup>	19.8
Nb	19.0	0.662	0.11	18.8 <sup>d</sup>	31.6
Mo	28.3	0.737	0.12	28.8 <sup>d</sup>	42.9
W	28.9	0.739	0.16	28.9 <sup>e</sup>	50.7
Ir	44.5	0.281	0.25		40.1
Pt	34.1	0.152	0.34		39.6
Au	18.6	0.163	0.33	22.5 <sup>c</sup>	23.2

<sup>a</sup>Reference 25.

<sup>b</sup>Reference 29.

<sup>c</sup>Reference 30.

<sup>d</sup>Reference 16.

<sup>e</sup>Reference 31.

23.1 GPa for Ni and Cu are lower than  $\sigma_{max,0}$  values (with allowed Poisson contraction) in Table II, in qualitative agreement with the above mentioned semiempirical calculations.<sup>28</sup>

Dependences for all the other crystals seem to be linear within the studied range of biaxial stresses. They can be parametrized as

$$\sigma_{max} = \sigma_{max,0} + k_{max}\sigma_{bi}, \quad (1)$$

where  $k_{max}$  is the slope expressing the influence of  $\sigma_{bi}$ . The parameters of a linear regression of computed data points are collected in Table II. Computed values of the slope  $k_{max}$  are mostly positive and seem to be higher for bcc crystals than for fcc ones. The only interesting exception of the studied elements is carbon in a diamond state, which exhibits a negative  $k_{max}$  and, thus, decreasing  $\sigma_{max}$  with increasing  $\sigma_{bi}$ . Its  $k_{max}$  value is about two times higher than that of bcc metals, but its value of  $\sigma_{max,0}$  is higher by an order of magnitude. The listed literature data for TTS were computed under the assumption of tensile instability (regardless of possible shear instabilities) and, thus, they should correspond to the  $\sigma_{max,0}$  values.

The result for Fe agrees well with TTS calculations of Clatterbuck *et al.*,<sup>10</sup> where the iron crystal was subjected to triaxial stress states with  $\sigma_{11}=2\sigma_{22}=2\sigma_{33}$  (superimposed tension) and  $\sigma_{11}=-\sigma_{22}=-\sigma_{33}$  (superimposed compression). Their uniaxial tensile strength of about 12.5 GPa matches the  $\sigma_{max,0}$  value in Table II. The strength value changed to about 18 GPa (8 GPa) when the authors applied the superimposed tension (compression), which is also in accordance with Eq. (1).

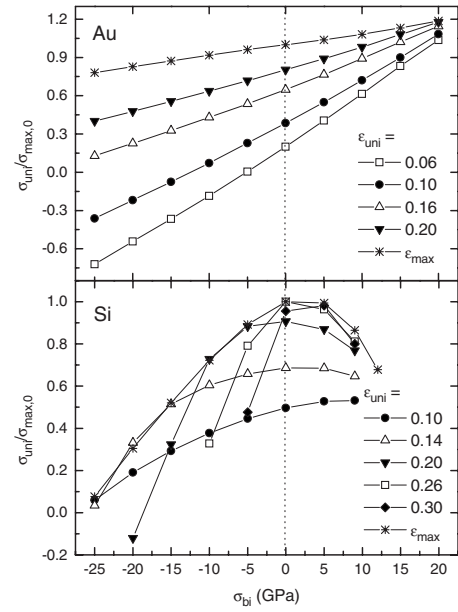


FIG. 2. Normalized values of [100] stress  $\sigma_{uni}/\sigma_{max,0}$  as functions of superimposed biaxial stresses  $\sigma_{bi}$  for several constant strain values  $\epsilon_{uni}$  (Si and Au).

### C. Stress-strain response

The influence of the biaxial stresses on the [100] tensile stress  $\sigma_{uni}$  remains qualitatively similar to that shown for  $\sigma_{max}/\sigma_{max,0}$  (Fig. 1 and Table II) also for [100] strain values smaller than  $\epsilon_{max}$ . This is demonstrated in Fig. 2 for particular cases of Au and Si crystals. All the curves related to different constant values of the [100] strain show the same trend. As can be seen for Au, the curves displaying the  $\sigma_{uni}(\sigma_{bi})$  dependence can be approximated by linear functions

$$\sigma_{uni} = \sigma_{uni,0} + k\sigma_{bi}. \quad (2)$$

However, the slope  $k$  decreases with increasing [100] strain  $\epsilon_{uni}$  ( $k=k_{max}$  for  $\sigma_{uni,0}=\sigma_{max,0}$ ).

Figure 3 displays the stress  $\sigma_{uni}$  as a function of  $\sigma_{bi}$  for several constant strain values  $\epsilon_{uni}$  for Mo in a more extended region of tensile biaxial stresses than that in Figs. 1 and 2. The dashed line defines the region of isotropic triaxial stress state ( $\sigma_{uni}=\sigma_{bi}$  and also  $\epsilon_{uni}=\epsilon_{bi}$ ) and the star represents a value of the theoretical isotropic strength  $\sigma_{iso}$  (see Table II). It can be clearly seen that the linear regressions (1) and (2) are just rough approximations, holding only for a rather limited range of tensile biaxial stresses. The deviation from the linear trend is particularly obvious for higher  $\epsilon_{uni}$  values. Theoretically, the function for  $\epsilon_{max}$  must approach the point related to the isotropic strength.

Consequently, one can expect that functions  $\sigma_{uni}(\sigma_{bi})$  exhibit maximum also for other crystals. The dependence can be reasonably linearized only in cases when the maximum of the function is well beyond the range of interest. Obviously, the dependence must have a maximum when  $k_{max} > 1 - \frac{\sigma_{max,0}}{\sigma_{iso}}$ .

Unlike for other crystals, extended calculations for diamond (in both tensile and compressive regions) also revealed

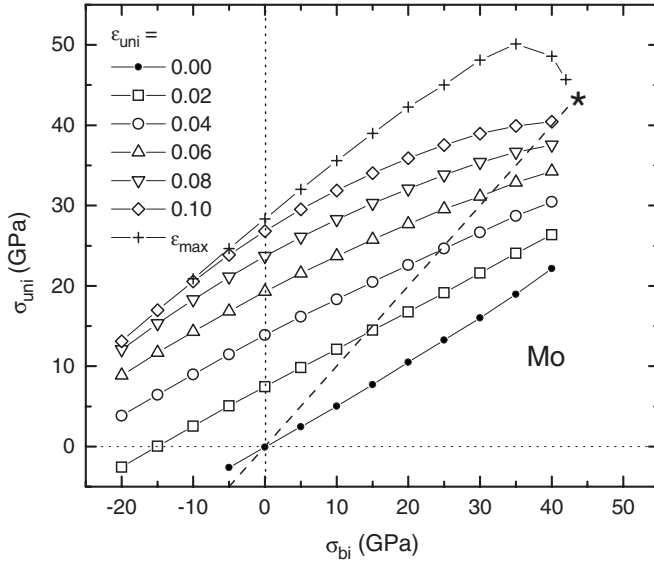


FIG. 3. The [100] tensile stress  $\sigma_{uni}$  as a function of the superimposed biaxial stresses  $\sigma_{bi}$  for several constant strain values  $\varepsilon_{uni}$  (Mo) and a more extended tensile range of  $\sigma_{bi}$ . The dashed line corresponds to states of cubic symmetry and the star to the theoretical isotropic strength  $\sigma_{iso}$ .

a maximum at compressive stress of about 120 GPa (see Fig. 4). The fact that only diamond strengthens under increasing transverse compressive stresses explains the opposite slope of the dependence in the studied range of  $\sigma_{bi} = \pm 25$  GPa.

Figure 3 also suggests how to estimate the slope  $k$  of  $\sigma_{uni}(\sigma_{bi})$  lines at constant small  $\varepsilon_{uni}$  values. In that case, the relations  $\sigma_{uni,0} = E_{100}\varepsilon_{uni}$  and  $\sigma_{iso} = B(v-1)$  are valid, where  $B$  is the bulk modulus and  $v = (1 + \varepsilon_{uni})^3$  is the relative volume. Then the  $k$  value can be roughly calculated from elastic moduli as

$$k = \frac{\sigma_{iso} - \sigma_{uni,0}}{\sigma_{iso}} \doteq 1 - \frac{E_{100}}{3B} = \frac{2C_{12}}{C_{11} + C_{12}}. \quad (3)$$

For example, when computing the  $k$  values of Mo for  $\varepsilon_{uni} = 0$  via linear regression of  $\sigma_{uni}(\sigma_{bi})$  data points and, simul-

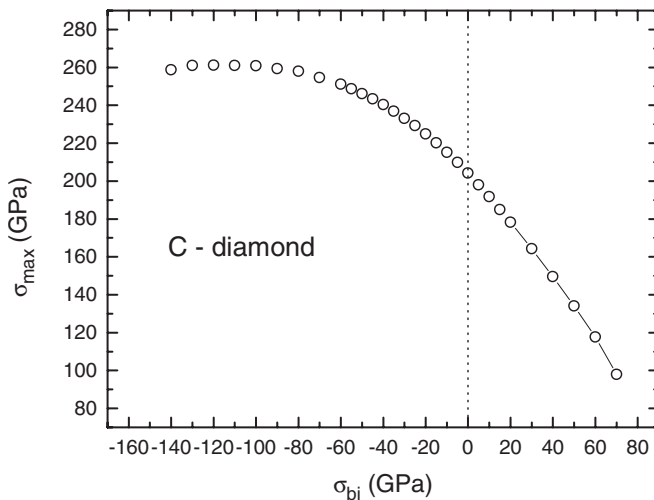


FIG. 4. The maximum tensile stress  $\sigma_{max}$  as a function of the superimposed biaxial stresses  $\sigma_{bi}$  for diamond in a more extended range of compressive  $\sigma_{bi}$ .

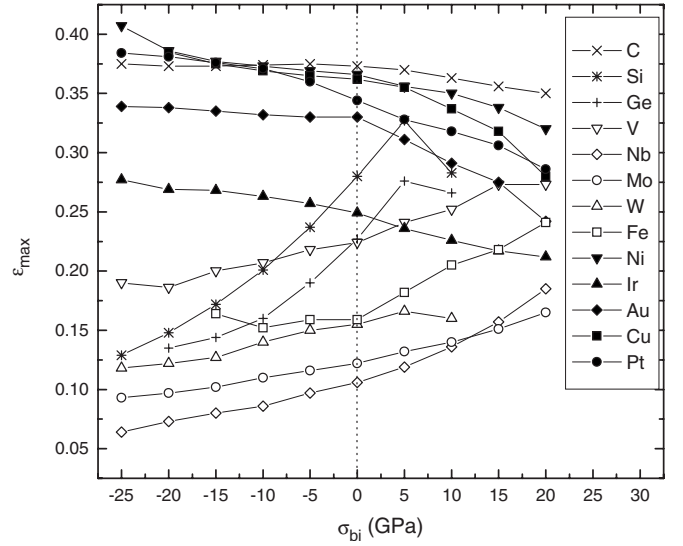


FIG. 5. The ultimate strain (elongation to failure)  $\varepsilon_{max}$  as a function of  $\sigma_{bi}$  for all the studied crystals.

taneously, by using Eq. (3) with experimental elastic constants, we obtain values of 0.516 and 0.514, respectively. Similarly computed values for Au of 0.913 from linear regression and 0.914 from Eq. (3) also match each other.

In other words, all dependences calculated for the tensile instability at  $\sigma_{max}$  can be qualitatively transferred also to points of shear or phonon lattice instabilities that could eventually occur in individual crystals. This is a very important result allowing a direct application of computed results to the assessment of the multiaxial strength of whiskers in the composite materials.

The ultimate strain  $\varepsilon_{max}$  (related to  $\sigma_{max}$ ) as a function of the biaxial stress is depicted in Fig. 5 for all crystals. As can be seen, the ultimate strains  $\varepsilon_{max}$  of fcc metals and diamond C decrease with increasing biaxial stress, whereas in the case of bcc metals and other two crystals of a diamond structure, they exhibit an increasing dependence on  $\sigma_{bi}$ . This result is qualitatively different from the behavior of crystals (or polycrystals) containing lattice defects and micropores. All these materials exhibit an exponential decrease of the ultimate (plastic) strain with increasing tensile biaxiality.<sup>32</sup> It clearly documents that the intrinsic deformability of a perfect crystal lattice does not determine the ductility of engineering crystalline materials.

#### IV. CONCLUSIONS

Atomistic modeling of tension in the [100] direction of perfect crystals under superimposed biaxial transverse stresses was performed using *ab initio* calculations. The tensile stress was found to increase (decrease) with increasing tensile (compressive) biaxial stresses for most of the studied elements. In a certain range of the biaxial stresses, the dependence is almost linear, and the coupling of [100] stress and transverse plane stresses can be described by Eqs. (2) and (3) for small [100] strain values or by Eq. (1) and Table II for ultimate strain values related to the maximum tensile stress.

On the other hand, within the same range, results for C show a decreasing trend and some elements (Cu, Ni, Ge, and Si) exhibit a maximum of the function close to the zero value of applied biaxial stress. For all investigated crystals, the results remain qualitatively valid in the whole range of their tensile deformation. This allows a direct application of obtained theoretical data to the assessment of the multiaxial strength of whiskers.

The ultimate strain is a decreasing function of the transverse biaxial stress only for fcc crystals and diamond. The

opposite is true for bcc and other diamond crystals, which is in qualitative disagreement with the behavior of crystalline materials containing lattice defects.

#### ACKNOWLEDGMENTS

This research was supported by the European agency COST (Action P19) and the Ministry of Education and Youth of the Czech Republic under Grant No. OC 148.

\*cerny.m@fme.vutbr.cz

- <sup>1</sup>C. R. Krenn, D. Roundy, M. L. Cohen, D. C. Chrzan, and J. W. Morris, Jr., Phys. Rev. B **65**, 134111 (2002).
- <sup>2</sup>D. Xu, R. Yang, J. Li, J. Chang, H. Wang, D. Li, and S. Yip, Comput. Mater. Sci. **36**, 60 (2006).
- <sup>3</sup>M. Černý and J. Pokluda, Mater. Sci. Eng., A, doi:10.1016/j.msea.2006.09.159.
- <sup>4</sup>C. Schuch, J. Mason, and A. Lund, Nat. Mater. **4**, 617 (2005).
- <sup>5</sup>P. Šandera, J. Pokluda, L. G. Wang, and M. Šob, Mater. Sci. Eng., A **234-236**, 370 (1997).
- <sup>6</sup>M. Černý, P. Šandera, and J. Pokluda, Czech. J. Phys. **49**, 1495 (1999).
- <sup>7</sup>M. Černý, J. Pokluda, M. Šob, M. Friák, and P. Šandera, Phys. Rev. B **67**, 035116 (2003).
- <sup>8</sup>M. Černý and J. Pokluda, J. Alloys Compd. **378**, 159 (2004).
- <sup>9</sup>W. Li and T. Wang, J. Phys.: Condens. Matter **10**, 9889 (1998).
- <sup>10</sup>D. M. Clatterbuck, D. C. Chrzan, and J. W. Morris, Jr., Scr. Mater. **49**, 1007 (2003).
- <sup>11</sup>G. Kresse and J. Hafner, J. Phys.: Condens. Matter **6**, 8245 (1994).
- <sup>12</sup>G. Kresse and J. Furthmüller, Phys. Rev. B **54**, 11 169 (1996).
- <sup>13</sup>P. E. Blöchl, Phys. Rev. B **50**, 17953 (1994).
- <sup>14</sup>D. Vanderbilt, Phys. Rev. B **41**, 7892 (1990).
- <sup>15</sup>J. P. Perdew and Y. Wang, Phys. Rev. B **45**, 13244 (1992).
- <sup>16</sup>W. Luo, D. Roundy, M. L. Cohen, and J. W. Morris, Jr., Phys. Rev. B **66**, 094110 (2002).
- <sup>17</sup>F. Milstein and S. Chantasiriwan, Phys. Rev. B **58**, 6006 (1998).
- <sup>18</sup>M. Černý, M. Šob, J. Pokluda, and P. Šandera, J. Phys.: Condens. Matter **16**, 1045 (2004).
- <sup>19</sup>D. M. Clatterbuck, C. R. Krenn, M. L. Cohen, and J. W. Morris, Jr., Phys. Rev. Lett. **91**, 135501 (2003).
- <sup>20</sup>D. M. Clatterbuck, D. C. Chrzan, and J. W. Morris, Jr., Acta Mater. **51**, 2271 (2003).
- <sup>21</sup>J. Wang, S. Yip, S. R. Phillpot, and D. Wolf, Phys. Rev. Lett. **71**, 4182 (1993).
- <sup>22</sup>F. Milstein, J. Zhao, and D. Maroudas, Phys. Rev. B **70**, 184102 (2004).
- <sup>23</sup>F. Milstein, J. Zhao, S. Chantasiriwan, and D. Maroudas, Appl. Phys. Lett. **87**, 251919 (2005).
- <sup>24</sup>C. Kittel, *Introduction to Solid State Physics*, 8th ed. (Wiley, New York, 2005).
- <sup>25</sup>R. H. Telling, C. J. Pickard, M. C. Payne, and J. E. Field, Phys. Rev. Lett. **84**, 5160 (2000).
- <sup>26</sup>G. Simmons and H. Wang, *Single Crystal Elastic Constants and Calculated Aggregate Properties: A Handbook* (MIT, Cambridge, MA, 1971).
- <sup>27</sup>J. F. Nye, *Physical Properties of Crystals: Their Representation by Tensors and Matrices* (Oxford University Press, New York, 1985).
- <sup>28</sup>F. Milstein and B. Farber, Philos. Mag. A **42**, 19 (1980).
- <sup>29</sup>D. M. Clatterbuck, D. C. Chrzan, and J. W. Morris, Jr., Philos. Mag. Lett. **82**, 141 (2002).
- <sup>30</sup>S. Chantasiriwan and F. Milstein, Phys. Rev. B **53**, 14080 (1995).
- <sup>31</sup>M. Šob, L. G. Wang, and V. Vitek, Mater. Sci. Eng., A **234-236**, 1075 (1997).
- <sup>32</sup>J. R. Rice and D. M. Tracey, J. Mech. Phys. Solids **17**, 201 (1969).